Nanoscale Advances

ROYAL SOCIETY OF CHEMISTRY

REVIEW

View Article Online
View Journal | View Issue

Cite this: *Nanoscale Adv.*, 2020, **2**, 1760

Recent advancements in the applications of carbon nanodots: exploring the rising star of nanotechnology

Vishnu Sankar Sivasankarapillai,†[a] Arivarasan Vishnu Kirthi, †[b] Murugesan Akksadha,[c] Somasundaram Indu,[c] Udhayakumar Dhiviya Dharshini,[c] Janarthanan Pushpamalar [de] and Loganathan Karthik *[cf]

Nanoparticles possess fascinating properties and applications, and there has been increasing critical consideration of their use. Because carbon is a component with immaterial cytotoxicity and extensive biocompatibility with different components, carbon nanomaterials have a wide scope of potential uses. Carbon nanodots are a type of carbon nanoparticle that is increasingly being researched because of their astounding properties such as extraordinary luminescence, simplicity of amalgamation and surface functionalization, and biocompatibility. Because of these properties, carbon nanodots can be used as material sensors, as indicators in fluorescent tests, and as nanomaterials for biomedical applications. In this review, we report on the ongoing and noteworthy utilization of carbon quantum dots such as bioimaging tests and photocatalytic applications. In addition, the extension and future components of these materials, which can be investigated for new potential applications, are discussed.

Received 21st December 2019
Accepted 30th March 2020

DOI: 10.1039/c9na00794f

rsc.li/nanoscale-advances

1. Introduction

The study of nanotechnology has resulted in the introduction of various types of nanomaterials, which possess diversified properties that can lead to the production of intriguing properties. Carbon nanodots, also called carbon dots (hereafter denoted as C dots), are a class of carbon nanoparticles that function within a nanosystem. They have recently gained significant attention due to their feasible and varied synthesis methods, unique optoelectronic properties, and strong luminescent behavior.

Xu, *et al.*[1] discovered the fluorescent fraction, which was found to be carbon nanomaterial derived as a fraction obtained from the purification of carbon nanotubes and was characterized using atomic force microscopy. A transition of chemical and physical properties occurred when the material was converted from a bulk form to its nanoform.

Carbon nanodots are a novel class of nanomaterials smaller than 10 nm in size that possess intriguing changes in their physicochemical properties such as optical capabilities and solubility. Carbon dots are the latest forms of quantum dots, which are a luminescent carbon nanomaterial with zero dimensions. The surface characteristics can be effectively altered and morphed so that they can become appropriately utilized. These dots exhibit very intriguing characteristics that include fluorescence, a lack of biological toxicity, resistance towards photobleaching, and homogenous dispensability.[2–6]

The initial fabrication of C dots was performed by Xu, *et al.*[1] using electrophoretic purification of single walled carbon nanotubes (SWCNT), which is another nano-form of carbon that possesses significant cytotoxicity. The authors analyzed SWCNT prepared from arc discharge soot and identified C dots as the fluorescent component, which is present along with short carbon tubes. Since then, researchers have been focused on more feasible and inexpensive methods for the fabrication of C dots, which is a class of novel and more promising nanomaterial for different applications.

Sun and co-workers synthesized graphene nanodots from carbon soot with polyethylene glycol (PEG)-1500N using the oxidation passivation method. It was found that passivation or the passivated agent is an important link to increase the fluorescence of C dots. Therefore, passivation was considered to be an effective strategy to increase the emission efficiency of C dots, as reported by Sun, *et al.*[7] Recent studies suggest that the

[a]*Department of Chemistry, NSS Hindu College, Changanacherry, Kottayam, Kerala, 686102, India*

[b]*National Centre for Nanosciences and Nanotechnology, University of Mumbai, Vidyanagari, Santa Cruz (East), Mumbai, India*

[c]*Department of Biotechnology, Sri Shakthi Institute of Engineering and Technology, Coimbatore, TN, India. E-mail: lkarthik2006@yahoo.co.in; Tel: +91-9952545640*

[d]*School of Science, Monash University Malaysia, Jalan Lagoon Selatan, Bandar Sunway 47500, Subang Jaya, Selangor Darul Ehsan, Malaysia*

[e]*Monash-Industry Palm Oil Education and Research Platform (MIPO), Monash University Malaysia, Jalan Lagoon Selatan, Bandar Sunway 47500, Selangor Darul Ehsan, Malaysia*

[f]*Salem Microbes Private Limited, Salem, Tamilnadu, India*

† Equally contributed.

optical features of C dots arise from the linear optical response of the partially sp^2-hybridized carbon domains located on the sp^3-hybridized amorphous cores present on the surface of C dots, which was detailed by Tepliakov, *et al.*[8]

2. Synthetic strategies for C dots

In recent years, there have been large numbers of reports describing how to synthesize a wide assortment of C dots through both conventional chemical methods and green eco-friendly methods. Every one of these strategies attempts to improve the synthesis of C dots through techniques such as reducing the number of steps in the overall process and adopting biological reagents or products, which make the synthesis ecofriendly and cost-effective, with optimization of the reaction environment for controlling the size and properties of the end product.

There have been reports describing the successful use of naturally abundant materials for the preparation of C dots that exhibit excellent emission properties.[9] The major preparation routes of C dots can be broadly classified by considering the nature of the processes, which include chemical methods and biological (eco-friendly/green) methods (Fig. 1).

2.1. Chemical methods

The prominent techniques that have been reported for the synthesis of C dots are described with clear emphasis on the conventional top-down or bottom-up approaches utilizing chemical preparation methods. These methods are further classified as described below.

2.1.1. Electrochemical method. The influence of applied potential on the size of C dots has been investigated, along with the preparation. There are many reports depicting the synthesis of C dots using the electrochemical process, such as Bao, *et al.*,[10] who reported the electrochemical tuning of C dots, including their fluorescent behaviour. Deng, *et al.*[11] successfully developed C dots directly from low-molecular weight alcohols. This process involved the transition of alcohols into carbon particles in a basic medium through electrochemical carbonization.

Hou, *et al.*[12] reported a one-pot electrochemical synthesis of C dots that was used for the detection of mercury ions. Zeng, *et al.*[13] developed high-quality C dots that were able to strengthen their electrical output and exhibited excellent catalytic performance through a novel bio-electrochemical method.

2.1.2. Hydrothermal method. There has been interest in researching microwave-assisted hydrothermal methods for their feasibility of synthesis. Wang, *et al.*[14] used a microwave-assisted hydrothermal method to produce C dots with good luminescent properties using graphene oxide as the precursor. Recently, Zheng, *et al.*[15] reported another very rapid method using *N*-(β-aminoethyl)-γ-aminopropyl trimethoxysilane to suppress the quenching of fluorescence of the synthesized C dots.

Biomolecules are also used as a precursor for synthesis. Yang, *et al.*[16] used glucose to prepare fluorescent C dots in the presence of monopotassium phosphate. In this system, the monopotassium phosphate acted as a controlling factor for tuning the emission spectra. Similarly, Chen, *et al.*[17] reported an efficient hydrothermal method that used lignin for synthesis. Zhang, *et al.*[18] developed chiral C dots through a one-step hydrothermal method. The authors used cysteine (*cis*-form) and citric acid as the carbon source and also found that the C dots had the ability to influence the physiology of mung bean plants.

2.1.3. Microwave- and ultrasonic-assisted chemical synthesis. Microwave-assisted synthesis can be used to prepare hydrophilic, hydrophobic, or even amphiphilic carbon dots.[19] Mitra, *et al.*[20] reported a very simple one-step microwave-assisted synthesis of hydrophobic C dots from polyoxyethylene–polyoxypropylene–polyoxyethylene (PEO–PPO–PEO) block copolymer known as Pluronic F-68 (PF-68). Jaiswal, *et al.*[21] fabricated C dots using microwave-assisted caramelization of PEG. Here, glycol acted as both a carbon source and as a passivating agent for the C dots.

Similarly, Zhai, *et al.*[22] reported microwave-assisted pyrolytic methods between citric acid and amines. Ma, *et al.*[23] reported the ultrasonic synthesis of N-doped C dots using glucose as the precursor along with ammonium hydroxide. Dang, *et al.*[24] developed C dots on a large scale using an oligomer polyamide

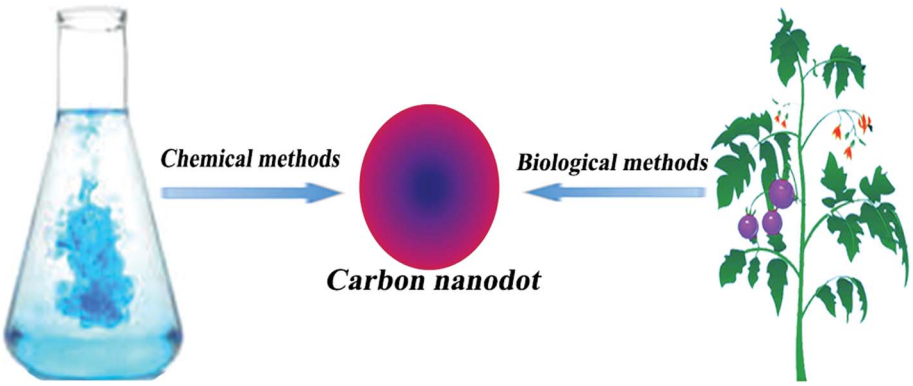

Fig. 1 Different methods used to prepare C dots.

resin as a carbon source and subjecting it to ultrasonic treatment.

2.1.4. Direct carbonization method. Direct pyrolysis (the pyrolytic method), which is the carbonization of carbon precursors under high temperatures, is a widely adapted method for the synthesis of C dots. It involves the utilization of strong acid or alkali to break down the precursors at the nanoscale. The carbonaceous source for this pyrolytic route can be waste peels of fruits, any type of juice, carbon-based compounds, or any material that has carbon present in it. In an example, Zhou and his co-workers reported the production of C dots prepared from fresh watermelon peel as the starting material. The peel was carbonized at 220 °C for 2 h, and the final product was purified using filtration and centrifugation. The particles were water-soluble with strong blue luminescence and were stable at different pH ranges.[25] The synthesis of C dots with high quantum yield and good water solubility, using citric acid and glutathione as the starting materials at 200 °C, was reported by Zhuo, *et al.*,[26] and these particles emitted blue-colored fluorescence with excitation-independent emission behavior. C dots can be induced or modified by adding ligands and subjecting the mixture to constant continuous stirring, or by introducing chemical bonds with either electrostatic interactions or amidation reactions.

The doping of heteroatoms can be utilized to alter the nanostructure of and electronic distribution in C dots. Nitrogen doping can be used for controlling fluorescence, and passivated surface states can be deduced using excitation independent behavior.[27–30] Additionally, hydrothermal carbonization methods have been described for the synthesis of N-doped carbon dots using bee pollen as the carbon source. The used route was very much ecologically green and was reported to yield 3 g of C dots from 10 g of raw material.

Wang, *et al.*[31] utilized a simple one-step approach for synthesizing C dots. The protocol consisted of 15 mL octadecene and 1.5 g of 1-hexadecylamine loaded in a three-neck flask and heated to 300 °C under argon flow. Then, 1 g citric acid was added to the solution under continuous stirring at 300 °C for 3 h, with subsequent purification by precipitation under acetone washing three times. The final product obtained was C dots that were highly soluble in common non-polar organic solvents.

2.2. Production of C dots from biological sources

It is desirable to synthesize C dots from precursors that are very much renewable, using naturally available raw materials and at low cost. An optimal synthesis route would be facile and would not require the use of harmful chemicals, but high temperatures or external energy for the production of the C dots would still be necessary, as shown in Fig. 2. The C dots synthesized from these raw materials possess properties and structures that are very much intriguing to researchers all over the world. The requirement of high reaction temperatures (100–200 °C) for the production of C dots is not necessary for synthesis using biological methods. The low cost of production and continuous availability of raw materials for the synthesis of C dots has made it a suitable protocol for industries. In addition, there is no requirement for the use of harmful organic solvents, but instead, aqueous solution can be prepared, and C dots prepared using this method exhibit increased water solubility.

Huang, *et al.*[32] summarized the primary preparation methods for C dots, which uses natural products as carbon sources for C dot synthesis. Zhu, *et al.*[33] used soy milk to fabricate C dots exhibiting both fluorescent behavior and oxygen reduction properties. Liu, *et al.*[34] used bamboo leaves, and the C dots were successfully applied for Cu(II) ion-sensing applications. Recently, Jayanthi, *et al.*[35] used edible carrots for C dot synthesis for imaging and catalytic applications. Because N-doped C dots are widely used, their green synthesis has also been well studied and reported. Wang and Zhou[36] provide an excellent example in which N-doped C dots were developed using milk and demonstrated utility for imaging applications. Recently, Mandal, *et al.*[37] reported the existence of N-doped carbon dots in human blood for the first time, which may be generated through the metabolic process of consumed food products.

3. Utilization and application of C dots

Nanoparticles are monomeric building blocks of nanotechnology and possess features such as strong bonds, delocalization of electrons with variation in size, and ability to make structural changes and affect physicochemical features ranging from melting points, electronic properties, magnetic properties, and surface charges. These particles have totally new and incremental properties compared to their bulk form due to changes in size and surface charges.

These properties of nanoparticles have led to the potential formation of nanodevices for target-specific and controlled delivery of biomolecules such as drugs, proteins, monoclonal antibodies, and nucleic acids. This will lead to drastic innovations in the field of cancer biology, vaccination, and other medical fields. Below are some of the fields where C dots have been developed and applied.

3.1. Bioimaging probes

Another interesting application of C dots is their utilization as a potential agent for the bioimaging of cells and species under *in vivo* and *in vitro* conditions due to their photoluminescence, which is an important property of C dots.[38] These particles have the ability to absorb UV light at the range of 270–320 nm, and can thereby assist in the presence of π–π^* and n–π^* electronic transition, which further proves the presence of conjugated systems and heteroatoms in C dots. In addition, these C dots produce interesting optical properties, *viz.*, phosphorescence, up-conversion photoluminescence, solid-state fluorescence, piezo-chromic fluorescence, and excitation-dependent emission.[39] The application of C dots in bioimaging *in vitro* and *in vivo* was first reported by Cao, *et al.*[40]

Bioimaging of cells and tissues is a vital part of the diagnosis of various diseases, especially cancer. There are various

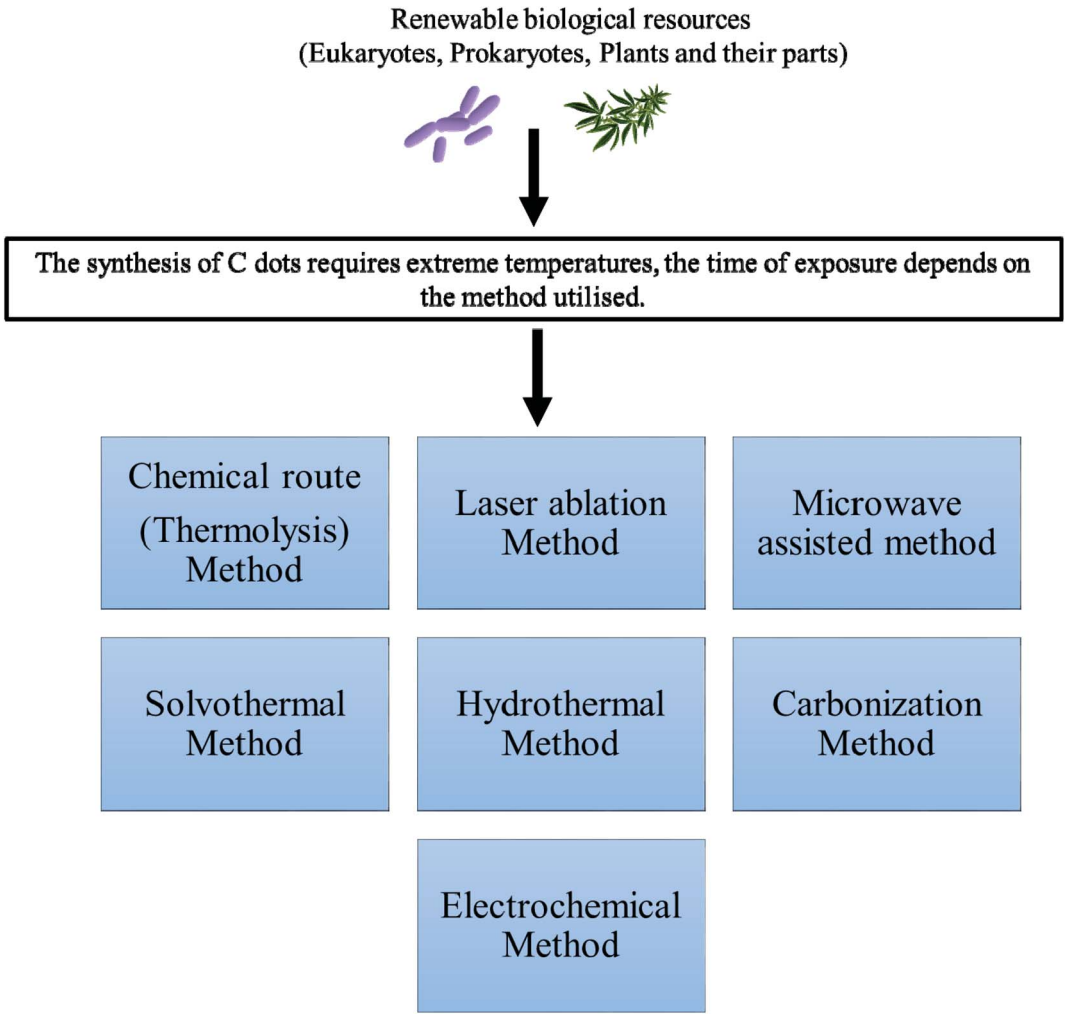

Fig. 2 Different routes for C dot preparation from biological sources.

fluorescent systems reported for diagnostic purposes starting from organic and inorganic dyes to the latest nanoparticle-based systems. The advantage of nanomaterials as imaging agents primarily depends on the lack of metal ion, which may adversely affect the *in vivo* environment *via* cytotoxicity pathways. With the advancement of nanotechnology, systems that are more diverse, such as quantum dot nanoparticles, have been reported for the imaging applications of living cells.

For a bioimaging agent to be considered suitable for use as an imaging probe, it must possess excellent biocompatibility, tunable emission spectra, and lack of cytotoxicity. The rapid progress in implementing a new class of nanoparticles has resulted in material that meets these criteria and can be simultaneously used not only for diagnosis but also for therapeutic applications. These theranostic applications are implemented by successfully conjugating the necessary drug molecule to the fluorescent nanoprobes through chemical functionalization. For instance, various biocompatible nanoparticles have been successfully reported in the literature for theranostic studies. Sivasankarapillai, *et al.*[41] provide a detailed account of silicon quantum dots (Si QDs), which are one of the widely explored nanoprobes for theranostic purposes. Si QDs have good biocompatibility because their chemical behavior is similar to that of carbon in the cellular environment. However, quantum dots (QDs) may possess some cytotoxicity, which may cause some adverse effects on the biological medium in which they were employed.

Sahu, *et al.*[42] reported the synthesis of C dots from the hydrothermal treatment of orange juice. This was one the initial examples of the preparation of fluorescent C dots from readily available natural resources. The C dots lacked cytotoxicity and exhibited efficient uptake by MG-63 human osteosarcoma cells for the purpose of cellular imaging. The same authors also developed a rapid live-cell mapping of a membrane decorated with sialic acid using poly-*p*-benzoquinone/ethylenediamine nanoclusters to form a structure that they called a wool ball. They synthesized sticky, furry, and fluorescent wool balls with diameters less than 2 nm, with abundant amino end groups. They were characterized, and the sialic acid expression was detected on the living cell surfaces within 30 min.

The genetic information flows from DNA to RNA to protein, which is called the 'central dogma'. Cheng and co-workers

examined the physiological activity of RNA in the course of cancer studies using RNA dynamics in cellular functions in the real-time monitoring of their temporospatial distribution. The experiments have been conducted using the developments of fluorescent carbon dots obtained from one-pot hydrothermal treatment of *o*-, *m*-, or *p*-phenylenediamines with triethylenetetramine. *In vivo* studies on zebrafish revealed the efficient and rapid excretion from the larval body within 48 h. This study assists in understanding RNA dynamics and basic biological processes, disease development, and drug interactions by Chen, *et al.*[43]

Because carbon is an element with exceptional biocompatibility and negligible cytotoxicity, there has been significant interest in using carbon nanodots as bioimaging probes over other classes of nanoparticles. Because of their ease of synthesis, satisfactory emission spectra, high photostability, and lack of cytotoxicity, C dots are ideal candidates for theranostic applications. Liu, *et al.*[44] developed C dots through a single-step process in which both formation and surface passivation of C dots proceed simultaneously. These C dots possess excellent biocompatibility and would be an ideal candidate for bioimaging due to their photoluminescent behavior, as shown in Fig. 3.

Liu, *et al.*[45] developed polyethyleneimine (PEI)-functionalized C dot-based nanocarriers for application in gene delivery and bioimaging probes. They act as a polyelectrolyte for condensation of DNA and also are a nitrogen-rich species, resulting in surface passivation and thereby increasing the fluorescence. Tao, *et al.*[46] developed C dots from carbon nanotubes (CNTs) and graphite through a mixed acid treatment. The C dots emit a strong yellow fluorescence under the UV range with no cellular toxicity. They also demonstrated the *in vivo* bioimaging property in the near-infrared region using a rat model, and this experiment exemplified the possibilities for the development of fluorescent imaging probes in both the UV and infrared (IR) range spectra.

The synthesis of C dots requires environmentally friendly routes of preparation, which is essential to make them cost-effective as imaging probes. Various methods for green synthesis have been reported for the fabrication of C dots considering the above concerns. Sahu, *et al.*[42] prepared C dots from orange juice in a single-step hydrothermal process. These C dots possessed qualities such as excellent biocompatibility and low cytotoxicity with a quantum yield of 26%, and were suitable for use as imaging probes. Chen, *et al.*[47] reported a high-yield single-step synthesis of C dots having a pH-independent photoluminescent intensity in the acidic and neutral range. They exhibited satisfactory stability and performed well for bioimaging applications.

Targeted drug delivery is a critical application that can be implemented with C dots. C dots can act as drug carriers and be monitored in real-time, making it feasible to utilize them due to their fluorescent behavior. Tang, *et al.*[48] developed a fluorescence resonance energy transfer-based C dot system for targeted drug delivery and monitoring. The authors demonstrated drug delivery efficiency using doxorubicin as the drug molecule and observed that there was satisfactory biocompatibility in the deep tissue environment. Aptamers have been reported as excellent candidates for targeted drug delivery due to their facile tethering of drug molecules. Lee, *et al.*[49] fabricated aptamer-conjugated C dots that were used for imaging cancer cells. The authors performed microwave-assisted synthesis using glycerol and mercaptoethanol for conjugating aptamers and C dots and explored their emission properties for bioimaging.

The role of functionalization in enhancing the properties of C dots has been thoroughly reviewed in the literature.[6] Recent works also focused on improving the efficiency of C dots by cross-linking with natural polymers such as nanocellulose.[50,51] This enables the development of biocompatible imaging systems based on C dots that can be used for gene therapy[52] and biomedical applications.[53] It was also recently reported that there were promising aspects of C dots that could be applied so that they would function as therapeutics for neurological disorders.[54]

3.2. Photodynamic therapy

Photodynamic therapy (PDT) is based on the combination of two components that are not cytotoxic. The two components are:

(1) Photosensitizer – a photosensitive molecule that can be localized in the biological environment of interest (cells/tissues).

(2) Activator (activated photosensitizer) – a component that activates the photosensitizer by implementing light transmission of a suitable wavelength.

The photosensitizer generates reactive oxygen species (ROS) by acting as a bridge that transfers energy from photons to molecular oxygen. The ROS species act as agents that mediate cytotoxic effects, and the action is limited only to specific target tissues that have been exposed to light. This light-induced toxicity is a tool that can be used to kill cancer cells or malignant tumors in a target-specific destructive action, as shown in Fig. 2. Dolmans, *et al.*[55] provide a detailed account of the application of PDT for cancer treatment. Recently, Kwok, *et al.*[56] reported a novel composition of PDT and imaging systems for various diseases including cancer (Fig. 4).

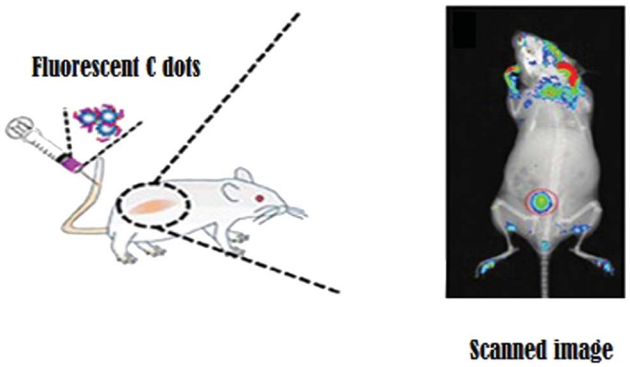

Fig. 3 *In vivo* imaging using fluorescent C dots.

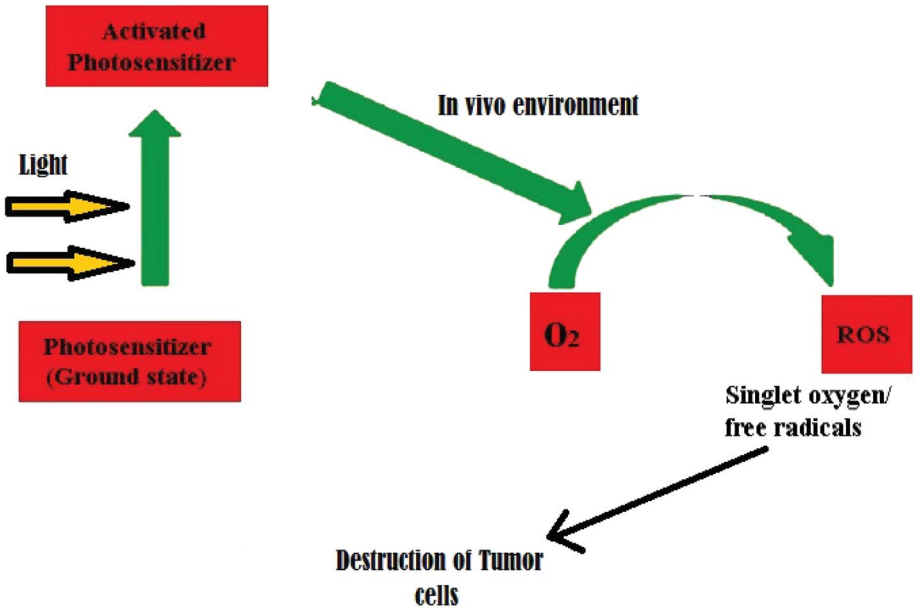

Fig. 4 Mechanism of photodynamic therapy in cancer treatment.

Photodynamic therapy is a recent advancement in biomedical nanotechnology whereby the energy transfer can be used to destroy damaged cells and tissues. This method is beneficial in dealing with cancer cells because it effectively targets the malignant tissue and destroys it without harming normal healthy tissue. This targeted destruction in photodynamic therapy can be successfully achieved using fluorescent C dots possessing satisfactory photostability. Choi, *et al.*[57] developed multifunctional C dots that can act as agents for both bioimaging and targeted photodynamic therapy in cancer cells. The authors verified the *in vitro* and *in vivo* potential of folic acid-modified C dots carrying zinc phthalocyanine acting as a photosensitiser.

Apart from *in vivo* imaging applications, the bioimaging of microorganisms has also been reported using C dots. Thakur, *et al.*[58] provide an excellent demonstration for these applications, where multifunctional C dots were conjugated with ciprofloxacin, a well-known antibiotic, and satisfactory microbial imaging activity was reported for the yeast *Saccharomyces cerevisiae*. This system can efficiently target the microbe and possesses enhanced antimicrobial activity with controlled drug–release properties. Zhang, *et al.*[30] employed rapeseed flowers and bee pollen to develop N-doped C dots using the hydrothermal method. After this successful large-scale synthesis, the authors demonstrated that C dots did not have a cytotoxic effect up to a limiting concentration of 0.5 mg mL^{-1}. In this work, human colon carcinoma cells were successfully imaged, and the C dots were found to have good photostability and biocompatibility.

Kuo, *et al.*[59] reported N-doped C dots having good biocompatibility and water solubility for *in vivo* bioimaging. These N-doped C dots possessed tunable fluorescence from 417 to 450 nm with a fluorescent quantum yield of 21.43%, which was significantly increased approximately 48% in comparison to that of C dots without nitrogen doping. Post-administrative fluorescence signal was observed in the lungs at 12 and 24 h in a rat model. The effect of N doping on bioimaging was quantitatively analyzed and reported. Wang, *et al.*[60] reported C dot synthesis from the condensation carbonization of linear polyethylenic amine (PEA) analogues and citric acid (CA) of different ratios. The authors successfully demonstrated that the extent of conjugated π-domains with C=N in the carbon backbone was correlated with their photoluminescence quantum yield. The main conclusion from this study is that the emission arises not only from the sp^2/sp^3 carbon core and surface passivation of C nanodots, but also from the molecular fluorophores integrated into the C dot framework. This work provided an insight into excellent biocompatibility, low cytotoxicity, and enhanced bioimaging properties of N-doped C dots, which opens the possibilities for new bioimaging applications.

A new possibility to overcome the limitation of conventional fluorescent imaging in biology is the introduction of super-resolution optical fluctuation bioimaging (SOFI). SOFI is a novel approach to develop high-quality bioimaging probes. The essential condition for SOFI is a requirement of two distinct fluorescent emission states, which can be attained through C dots. Dertinger, *et al.*[61] gives a detailed account of SOFI as a new platform for imaging possibilities in cell biology. The authors address SOFI as an effective and straightforward approach for bioimaging. Chizhik, *et al.*[62] successfully developed dual-color C dots having SOFI properties and good biocompatibility. The dual color is attributed to arise from two classes of charged species in the system. The neutral species act as probes for nuclei labeling, which opens the possibilities for developing nucleus-specific imaging agents for real-time applications.

Loukanov, *et al.*[63] developed C dots conjugated with fluorescein photosensitizer *via* the diazo bond. They exhibited lower

quantum yield but more optimal photostability toward emission quenching in cell culture. These photosensitizer-conjugated nanoprobes functioned as multifunctional candidates for *in vivo* imaging and tracers for labeling the endocytosis pathway in tobacco cells. They possess negligible cytotoxicity compared to conventional quantum dot probes for the same purpose. Aiyer, *et al.*[64] also successfully demonstrated similar bioimaging of cancer cells using C dots in an *in vitro* model. The authors used green fluorescent C dots approximately 3 nm in size that were modified with folic acid to improve their targeted conjugation to cancer cells. The folic acid group was efficiently targeted to the folate receptors present on the surface of malignant cells.

Apart from imaging, the therapeutic potential of C dots has been reported in the literature. Bankoti, *et al.*[65] fabricated C dots from onion peel powder waste using the microwave method and studied cell imaging and wound healing aspects. The C dots exhibited stable fluorescence at an excitation of 450 nm and emission wavelength at 520 nm at variable pH along with the ability to scavenge free radicals, which can be further explored for antioxidant activity. Radical scavenging ability leads to enhanced wound healing ability in a full-thickness wound in a rat model. Zhao, *et al.*[66] developed N and P co-doped red emissive C dots as efficient PDT agents using *o*-phenylenediamine and phosphoric acid as the raw materials. Recently, selective RNA binding to Se/N-doped carbon dots was developed as a photosensitizer for PDT.[67] Interesting results were also obtained for C dots conjugated with macromolecules such as protoporphyrin IX.[68]

The possibilities of C dots as fluorescent nanoprobes are unlimited, and scientists have only begun to explore their many uses. Multifunctional C dots exhibit great potential that should be explored in detail.[69] For instance, C dot imaging probes can serve as a nano-vehicle for targeted drug or gene delivery, antibacterial or antimicrobial carriers, and for wound-healing applications that have yet to be studied in detail. These features can be applied to new uses for biomedical research, and can resolve many of the barriers that exist in the present scenario.

3.3. Biological and chemical sensors

There is intense interest in the use of nanoparticles as biochemical sensors, as C dots have been found to be useful in sensing chemical compounds or elements. Different sensors for biological and chemical applications have been developed based on the properties of C dots, especially fluorescence properties and surface-functionalized chemical groups. For example, the detection of Hg^{2+} and biological thiols by C dots has been reported.[70]

With the advancement of C dots, their use as sensory probes to detect metal ions, organic compounds, and biomolecules has been thoroughly explored. The extensive research interest is due to the numerous features of C dots that are ideal for sensors because they include bright and intensive fluorescence emission in the visible range, quenching of fluorescence in the presence of target species, variable emission spectra, feasibility of preparation, and negligible cytotoxicity. The general working principle of a C dot-based sensor can be represented as shown in Fig. 5.

In many of the C dot sensors, an organic dye is conjugated that exhibits satisfactory fluorescent behavior. Shi, *et al.*[71] successfully developed a pH sensor based on dual-labeled C dots (DLCD) tethered with two fluorescent dyes, fluorescein isothiocyanate (FITC) and rhodamine B isothiocyanate (RBITC), for measuring intracellular pH. The authors additionally provide a significant observation that the molar feed ratio of FITC to RBITC is a critical factor for the pH response range of DLCD, and that a higher concentration of RBITC would decrease the sensitivity of the sensor. Kong, *et al.*[72] also reported a similar pH sensor based on two-photon fluorescence of C dots, which can detect the pH change at a depth of 65–185 μm in living cells. Zhu, *et al.*[73] reported the development of a nano-hybrid sensor system based on carbon dots and CdSe/ZnS quantum dots with *N*-(2-aminoethyl)-*N*,*N*′-tris(pyridin-2-yl-methyl)ethane-1,2-diamine (AE-TPEA) acting as a recognition molecule. This sensor successfully detected copper(II) ions by the quenching of fluorescence. Sha, *et al.*[74] reported a similar detection of copper(II) ions using nitrogen-containing C dots. The authors prepared C dots using a hydrothermal method, and they exhibited strong blue luminescent emission at 450 nm when excited at 369 nm.

In past decades, there has been increasing interest in aptamers as drug delivery agents. There are many studies showcasing hybrid sensors based on a C dot-aptamer system for the fluorescence detection of biomolecules. Xu, *et al.*[75] reported such a sensor system for the detection of thrombin, with a reasonable detection limit of 1 nM. This sensor was composed of C dots functionalized with aptamers and possessed excellent biocompatibility and negligible cytotoxicity. Here, the structural fluctuation of the sensor into sandwich geometry upon interaction with thrombin caused fluorescence variation. Fe(III) is a metal ion that is widely explored with C dot sensors.

Qu, *et al.*[76] designed and prepared ratio-metric fluorescent nano-sensors using C dots through a single-step microwave-assisted synthesis. This work is very significant in C dot sensor research because the developed nanosensors possess multi-sensory capacity and can detect temperature, pH, and metal ions such as Fe(III). This exciting feature is proving to be widely applicable in the biological environment because it can simultaneously detect and estimate various metabolic parameters. The sensory mechanism is based on ratiometric fluorescence, and is non-cytotoxic, which is a promising feature for further research.

C dots can also detect other inorganic metal ions such as tin(II) ions in aqueous medium. Mohd Yazid, *et al.*[77] reported a sensor probe based on C dots that was prepared using a green synthetic strategy. The authors employed starch nanoparticles for the preparation of C dots through surface oxidation and carbonization. The probe exhibited excellent selectivity with minimal chemical interference from other species. Furthermore, the sensing mechanism was found to be the quenching of fluorescence by Sn(II) ions, with a detection limit of 0.36 μM. A similar sensor was developed for Hg(II) ions with a detection

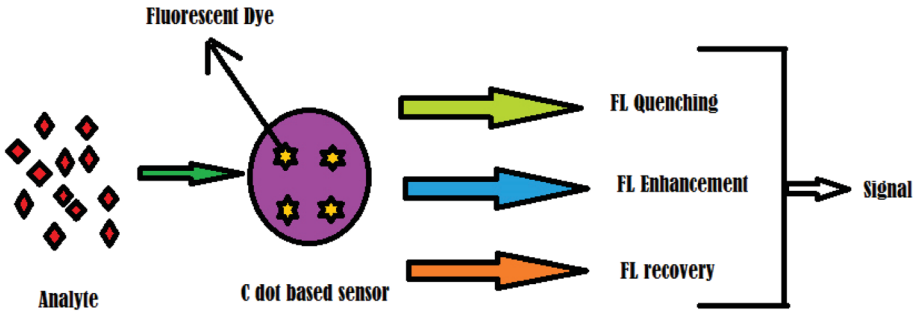

Fig. 5 Principle of C dot-based sensors.

limit as low as 0.5 nM. Furthermore, the authors successfully employed it for the detection of Hg(II) in lake water samples. Similarly, a C dot sensor combined with metal complexes was also reported for Hg(II) detection.[78]

Yuan, *et al.*[79] reported a good example of this type of sensor, which contained C dots functionalized with a bis(dithiocarbamato)copper(II) complex ($CuDTC_2$). Similar work was reported by Noh, *et al.*,[80] who described a self-delivering C dot-based sensor for the detection of microRNA. The authors developed C dots from candle soot through thermal oxidation. The sensory mechanism involved restoring the fluorescence of the sensor probe through the detachment of quencher, and it was observed to have functional specificity for microRNA 124a, which is highly expressed in neurogenesis. The material exhibited no toxicity, more optimal self-luminescence, and highly self-driven cellular uptake, which indicate that the detection of various other diseases associated with miRNAs is feasible, effective, and accurate.

C dots developed through cost-effective methods have been used for sensory applications. Tan, *et al.*[81] successfully developed C dots from industrial sago waste and applied them to the sensing of various metal ions. They adopted a single step pyrolytic method for the fabrication and optimized the carbonization temperature. Vedamalai, *et al.*[82] successfully developed C dots for highly sensitive detection of copper(II) ions in cancer cells. They adopted a comparatively simple synthesis method based on a hydrothermal method using *ortho*-phenylenediamine (OPD). The formation of the $Cu(OPD)_2$ complex on the surface of C dots changed the yellow color to orange. Further investigation revealed that the C dots exhibited high water dispersibility, photostability, chemical stability, and excellent biocompatibility.

Shi, *et al.*[83] also reported C dots for the detection of Cu(II) ions in living cells. The pyrolysis of leeks using a hydrothermal method produced blue and green florescent C dots. The C dots were modified with boronic acid through a single-step hydrothermal carbonization, using phenylboronic acid as the precursor. Blood sugar sensing was successfully performed using this C dot-based sensor, and it exhibited good selectivity with minimal chemical interference from other species.[84] The sensing pathway was analogous to other sensing processes in which the quenching of C dots takes place *via* glucose binding. This work indicated the possible development of a simple but efficient blood glucose monitoring system for real-time applications.

Apart from metal ions, other biological factors such as pH and hemoglobin have also been successfully detected using C dot-based sensors. Nie, *et al.*[85] developed a pH sensor from C dots using a novel bottom-up approach. This method produced C dots with good crystallinity and high stability. The process involved a one-pot synthesis using chloroform and diethylamine with high reproducibility. The authors successfully implemented the pH detection of two C dots with different emission wavelengths and were able to use the technique for cancer diagnosis.

Wang, *et al.*[86] reported an interesting C dot sensor for the detection of hemoglobin (Hb). The C dots were prepared from glycine through the electrochemical method, and the development involved the multistep processes of electro-oxidation, electro-polymerization, carbonization, and passivation. The authors successfully validated the sensitivity of Hb detection and observed that the luminescence intensity inversely varied with Hb concentration over the range of 0.05–250 nM. The process of detection occurred through fluorescence resonance energy transfer (FRET) phenomena, and the C dots exhibited excellent chemical stability. It has also been reported that C dots have been used as sensory nanozymes in biological environments. Mohammadpour, *et al.*[87] developed such a sensitive probe that was used as a colorimetric sensor for the Hg(II) ion. The authors employed cysteine as a molecular agent to form a complex with mercury, in which case, the sensor was turned off, and it was observed to have a detection limit of 23 nM.

Zhang, *et al.*[88] also reported a C dot-based sensor for the selective detection of Fe(III) ions. This work explored the idea of tuning the photoluminescence of C dots through the tuning of the passivating reagents in the synthesis step. Sweet potato has also been used as a precursor for C dot synthesis. Shen, *et al.*[89] developed such a sensor for detecting Fe(III) with cell imaging applications. Kim, *et al.*[90] developed an aluminum(III) ion sensor based on C dots conjugated with a rhodamine 6G moiety. This paper-based sensor selectively detected Al(III) ions in the presence of other metal species. The sensing mechanism is based on the energy transfer process in which the Al^{3+}-induced ring opening of rhodamine on C-dots through the chelation of the rhodamine 6G moiety with Al(III) resulted in the spectral overlap

of the absorption of C-dots (acting as a donor) and the emission of ring-opened rhodamine (acting as an acceptor).

Chen, *et al.*[91] aimed to detect guanosine 3′-diphosphate-5′-diphosphate, which plays a pivotal role in plants and bacteria in gene expression, rRNA, and antibiotic production for the growth of plants. They synthesized C dots with terbium ions, resulting in a stable, narrow emission and excitation wavelength-independent emission with the limit of detection at 50 nM based on the synergistic effect of Tb^{3+} ions. Chen, *et al.*[92] synthesized graphene quantum dots (average size 4.5 ± 2.5 nm) using hydroquinone with hydrogen peroxide that was reacted with triethylenetetramine.

Gong, *et al.*[93] developed N-doped C dots that could effectively detect ferric(III) ions, as well as be used for cellular imaging. They adopted a method of microwave-assisted synthesis of C dots using chitosan as the carbon source, acetic acid as the condensation agent, and 1,2-ethylenediamine as the N-dopant. It was observed that N doping increased the fluorescence emission and assisted in the detection of Fe(III) ions through quenching. The detection limit was observed to be at the 10 ppb level. N-doped C dots have also been used for the detection of mercury ions.

Wang, *et al.*[94] reported a fascinating work in which a portable mercury-sensing C dot was developed from chitosan, and the detection was performed through a smartphone application. Here, the N-doped C dots exhibited a high quantum yield (31.8%) because of nitrogen incorporation coincident with multiple types of functional groups (C=O, O–H, COOH, and NH_2). This work was the first to report the detection of a heavy metal ion through electronic application along with cellular imaging.

Zhang, *et al.*[95] reported N-doped C dots for the detection of 2,4,6-trinitrotoluene (TNT). Here, the sensor acted as a dual detection system through both electrochemical and fluorescent methods. The sensor was precise and selective, with up to nM concentration sensitivity. Cayuela, *et al.*[96] also reported a similar C dot-based sensor for the detection of explosives derived from an amphiphilic polymer dodecyl-*grafted*-poly(isobutylene-*alt*-maleic-anhydride) through a single-step process. The authors successfully conducted the detection of TNT and 2,4-dinitrotoluene (2,4-DNT) and its related byproducts (mono- and dinitro aromatic compounds) in soil samples.

C dot-based sensors successfully detected similar TNT compounds as well as other organic compounds. Wu, *et al.*[97] recently constructed a sensor array system using three types of Ag(I) ion-sensitive C dots for the detection of biothiols. This work indicates the possibility of constructing additional C dot sensors for biologically significant organic moieties and metabolites.

Many other works have been reported that involved sensors based on N-doped C dots. Huang, *et al.*[98] prepared a similar non-cytotoxic N-doped C dot sensor *via* a one-pot microwave-assisted hydrothermal method using histidine as the carbon source. This sensor could detect Fe(III) ions in living cells with a detection limit of 10 nM and was also able to penetrate cancer cells. N-doped C dots prepared from natural precursors have also been reported for sensory applications. Edison, *et al.*[99] reported a good example of such a procedure in which an extract of *Prunus avium* fruit was used for preparation. This method was inexpensive, with much potential for further development.

In addition to Fe(III), it has been reported that other heavy metals can be detected by N-doped C dot sensor probes. Wen, *et al.*[100] reported a similar work involving a green synthesis utilizing a hydrothermal method in which pigskin was used as the precursor. The sensor exhibited a good response to cobalt(II) ions through fluorescence quenching and was used to quantitatively detect Co(II) in living cells. Cui, *et al.*[101] reported a N and S co-doped C dot sensor for detecting Fe(III) ions, which is an example of a co-doped sensory system for metal ion sensing.

Yan, *et al.*[102] reported a C dot sensor for detecting Al(III) and dopamine also utilizing a simple one-step hydrothermal preparation method. The C dots exhibited excellent water solubility with negligible cytotoxicity. Pang, *et al.*[103] developed a C dot sensor for the detection of guanine. Here, the authors used non-functionalized C dots for the selective detection of guanine in urine and DNA samples, with a detection limit of 0.67×10^{-8} mol L^{-1}. Novel solvent-free methods have also been reported for preparing C dot sensors using protocols other than conventional synthetic methods.

Iqbal, *et al.*[104] reported a novel solid-state synthesis of C dots using citric acid and phenanthroline. This method was very cost-effective and can be used for detecting both Fe(II) and Fe(III) present in cells and milk, with a detection limit of 20 nM and 35 nM for Fe(II) and Fe(III), respectively. Recent studies have reported the successful fabrication of highly efficient C dots through feasible methods. The C dots can be used as sensors for various biologically significant molecules such as tetracyclines,[105–107] epinephrine,[108] ampicillin,[109] penicillin G,[110] acetamiprid,[111] glutathione,[112] and also for organic molecules such as catechol,[113] toluene,[114] biothiols,[115] thioamides,[116] and also for microbes such as *Pseudomonas aeruginosa* bacteria.[117]

3.4. Photocatalysis

There has been significant research interest in photocatalysts over the past decade due to the scenario of environmental safety and sustainable energy. The applications of nanomaterials for efficient fabrication of photocatalysts made the journey fast and effective. It has been reported that C dots have been developed as useful photocatalysts for the degradation of organic dyes and also for the photo-splitting of water for hydrogen generation, as shown in Fig. 6.

Ming, *et al.*[118] successfully developed C dots through a one-pot electrochemical method using only water as the major reagent. This is a very promising synthetic methodology because it is a green protocol and is cost-effective, with good photocatalytic activity of C dots for the degradation of methyl orange. Furthermore, when the C dots were coupled with titanium dioxide (TiO_2), they exhibited excellent photocatalytic efficiency.

It was previously observed in past decades that the *Z*-scheme photocatalysts possessed enhanced catalytic efficiency. Zhou, *et al.*[119] provides a detailed account for these solid-state *Z*-

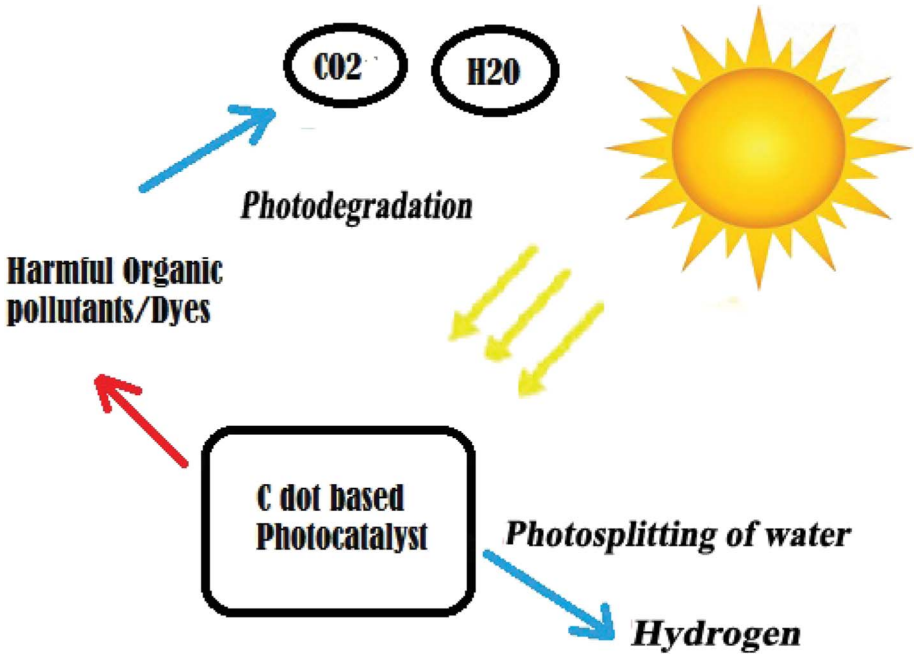

Fig. 6 Principle of C dot-based photocatalysts.

scheme photocatalytic systems. A *Z*-scheme-based system was applied to C dot-based photocatalysts and was observed to have good efficiency. Similarly, it was observed that the C dot/WO_3 *Z*-scheme photocatalysts for hydrogen production exhibited good efficiency. With xenon lamp irradiation, it was demonstrated that the rate of hydrogen production increased from 4.65 mmol g^{-1} h^{-1} to 1330 mmol g^{-1} h^{-1}.[120]

An excellent extension of this system operating in the broad spectrum range was reported in the literature. A *Z*-scheme composite composed of a C dot/WO_3 nanorod system demonstrated its efficiency in broad spectrum photocatalysis using ultraviolet-visible (UV-Vis) and near-infrared (NIR) irradiation.[88] The authors reported reaction rate constants of 0.4030 and 0.2889 h^{-1} for the photo-oxidation of tetracycline hydrochloride (TCH) and phenol, respectively, which were approximately 2.9-fold higher than those for bare WO_3 nanorods due to the synergistic effect.

A similar *Z*-scheme photocatalyst was recently reported for a hydrogen evolution reaction using MoS_2 QDs decorated with *Z*-scheme graphitic carbon nitride (g-C_3N_4) nanosheet/N-doped carbon dot heterostructures[121] and a nitrogen-doped C dot/$CuBi_2O_4$ microrod composite.[71] Band gap tuning and surface modification were reported as effective protocols for fabricating C dots with excellent performance in photocatalysis.[122]

Gao, *et al.*[123] provide detailed insight into the molecular mechanism of the C dot/g-C_3N_4 system using density functional theory (DFT). The authors explain the interaction between C dots and g-C_3N_4 through the formation of a type-II van der Waals heterojunction, which leads to a decrease in band gap. Furthermore, this work demonstrated that the C dots act as a spectral sensitizer in the system, which assists in the photocatalytic splitting of water. Park, *et al.*[124] introduced C dot-based fluorescent paint with photocatalytic activity. The authors prepared C dot paint from PEG through ultrasound irradiation, and it was found to have a quantum yield of nearly 14%. This material was also observed to be capable of detoxifying organic dyes when incorporated in the photocatalytic TiO_2 system. Further studies will be beneficial for the development of effective water purification systems based on this property.

Previous studies showed that C dots alone can also be used for photocatalytic hydrogen production without any co-catalysts or modification. Yang, *et al.*[125] reported such a work that used pure C dots for hydrogen generation through photolysis. The authors observed that the hydrogen production reached a value of 3615.3 μmol g^{-1} h^{-1} using methanol as the sacrificial donor. This efficiency is very promising because it is 34.8 times higher than that of the commercial Degussa P25 titania photocatalyst under the same conditions.

Song, *et al.*[126] designed a two-step hydrothermal method for developing a C dot-WO_2 photocatalyst. The authors employed this system for the photocatalytic degradation of rhodamine B. It is worth mentioning that this work reports a reaction rate constant of 0.01942 min^{-1}, which is approximately 7.7 times higher than the catalytic rate using WO_2 alone. This sizeable increase in the catalytic rate is attributed to the synergistic mechanism of C dots and WO_2, causing improved light-harvesting ability and excellent spatial separation of photo-excited electron–hole pairs. Furthermore, the photocatalytic action of C dots in rhodamine B under UV irradiation is also affected by pH variation, which also occurs with photoluminescence. The authors reported that maximum photocatalytic efficiency was observed at pH 1 due to the formation of hydrogen bonds.[120]

A C dot/(g-C_3N_4) system has been used for photocatalytic hydrogen generation. The authors prepared C dots from rapeseed flower pollen and incorporated them into g-C_3N_4 through the hydrothermal method. This system was able to photocatalytically generate hydrogen *via* sound with an output that was 88.1 μmol h^{-1} times greater than that of bulk g-C_3N_4 under visible light irradiation.[127] Other works also reported exploring the molecular mechanism of photocatalytic action of the C dot/g-C_3N_4 system.

Recently, the hybrid C dot/protonated g-C_3N_4 system was used to study the photoreduction of CO_2 into CH_4 and CO using both experimental and DFT methods.[128] It was observed that this hybrid system was very effective in the photoreduction of CO_2 with good stability and durability after four reaction cycles. DFT calculations were consistent with the experimental results, which implies that the work function of C dots (5.56 eV) was larger than that of pCN (4.66 eV). This suggests that the efficient shuttling of electrons from the conduction band of protonated g-C_3N_4 to C dots hampers the recombination of electron–hole pairs. This process enhanced the probability of free charge carriers reducing CO_2 to CH_4 and CO, giving satisfactory efficiency for photoreduction.

The performance of these systems has also been improved by incorporating Fe(III) ions. Researchers who grafted Fe(III) ions to the surface of a C dot-Fe doped g-C_3N_4 system validated the improvement in photocatalytic efficiency.[127] This work revealed that the interfacial charge transfer effect (IFCT) effectively inhibited charge recombination and resulted in satisfactory photocatalytic activity. Furthermore, the authors revealed that the incorporation of Fe(III) produced hydroxyl radical (OH*), which plays a crucial role in the photodegradation of methyl orange and phenol.

The application of a co-catalytic system can significantly improve the functions of photocatalytic applications compared to bare C dots. Zhang, *et al.*[129] used a co-catalysis system consisting of a C dot-Co_3O_4–Fe_2O_3 photo-anode for the photooxidation of water. The authors observed that a photocurrent density of 1.48 mA cm^{-2} at 1.23 V was exhibited by this ternary co-catalytic system, which was 78% higher than that of the bare Fe_2O_3 photo-anode. Aggarwal, *et al.*[130] prepared C dots from bitter apple peel and demonstrated visible light photocatalytic activity for the degradation of crystal violet. A similar result was observed for C dots prepared from palm powder.[131]

The possibilities for using C dots to develop efficient photocatalysts with good efficiency and low cost are very vast. Recently, methylene–oxygen bond-reductive photocleavage in *N*-methyl-4-picolinium esters was performed using C dots.[132] The literature suggests that structural features affect the photocatalytic performance of C dots,[133] while an interfacial reaction also plays a key role in C dot-based nanocomposites.[1] More importance is to be given to hybrid C dot-based photocatalytic systems, which increase efficiency when combined with co-catalysts and other inorganic materials. Apart from these, polymers can also be incorporated, which increase the flexibility and cost-effectiveness of the system, and these aspects require further research.

4. Scope and future perspectives

Various factors such as comparatively feasible synthesis and excellent biocompatibility indicate that a nanomaterial is suitable for biological applications and possesses tunable optical and electronic properties. Based on these criteria, C dots are ideal candidates because of their unique potential to be applied in research. In the past decades, there has been enormous research interest in C dots due to their ideal behavior, which continues to be explored.

Further experimentation is ongoing in the application of C dots as drug carriers for targeted drug delivery, with continued exploration of their enhanced blood–brain barrier permeation ability and theranostic properties so that they can be useful in therapies against advanced diseases and disorders. This can open new opportunities for their use so that they can be successfully substituted in applications where traditional nanomaterials failed.

5. Conclusion

Carbon-based nanomaterials are of great interest to nanotechnologists due to their fascinating behavior and great potential for various optical, electronic, and *in vitro* and *in vivo* applications. This broad acceptance of carbon nanomaterials depends primarily on their comparatively feasible preparation methods and the proper tuning of their desired properties. This review addressed the three major applications of C nanodots: bioimaging, photocatalysis, and sensors. These strategies exploit the unique features of C dots such as biocompatibility, fluorescence behavior, and feasible synthetic protocols. We anticipate that this review will provide valuable insight regarding the properties of C dots, and will assist researchers to move forward and explore the hidden potential of C dots, advance the current research, and implement further applications of this unique class of nanomaterials.

Conflicts of interest

The authors declare no conflict of interest.

Acknowledgements

The authors thank the management of the Sri Shakthi Institute of Engineering and Technology, Coimbatore, Tamil Nadu, India.

References

1 X. Xu, R. Ray, Y. Gu, H. J. Ploehn, L. Gearheart, K. Raker and W. A. Scrivens, *J. Am. Chem. Soc.*, 2004, **126**, 12736–12737.
2 Y. Zhou, D. Benetti, X. Tong, L. Jin, Z. M. Wang, D. Ma, H. Zhao and F. Rosei, *Nano Energy*, 2018, **44**, 378–387.
3 J. Xu, Y. Miao, J. Zheng, H. Wang, Y. Yang and X. Liu, *Nanoscale*, 2018, **10**, 11211–11221.
4 L. Hu, H. Li, C. Liu, Y. Song, M. Zhang, H. Huang, Y. Liu and Z. Kang, *Nanoscale*, 2018, **10**, 2333–2340.

5 C. Liu, Y. Fu, Y. Xia, C. Zhu, L. Hu, K. Zhang, H. Wu, H. Huang, Y. Liu, T. Xie, J. Zhong and Z. Kang, *Nanoscale*, 2018, **10**, 2454–2460.
6 B. B. Chen, M. L. Liu, C. M. Li and C. Z. Huang, *Adv. Colloid Interface Sci.*, 2019, **270**, 165–190.
7 Y. P. Sun, B. Zhou, Y. Lin, W. Wang, K. A. Fernando, P. Pathak, M. J. Meziani, B. A. Harruff, X. Wang, H. Wang, P. G. Luo, H. Yang, M. E. Kose, B. Chen, L. M. Veca and S. Y. Xie, *J. Am. Chem. Soc.*, 2006, **128**, 7756–7757.
8 N. V. Tepliakov, E. V. Kundelev, P. D. Khavlyuk, Y. Xiong, M. Y. Leonov, W. Zhu, A. V. Baranov, A. V. Fedorov, A. L. Rogach and I. D. Rukhlenko, *ACS Nano*, 2019, **13**, 10737–10744.
9 J. Mathew, J. Joy and J. Philip, *J. Lumin.*, 2019, **208**, 356–362.
10 L. Bao, Z. L. Zhang, Z. Q. Tian, L. Zhang, C. Liu, Y. Lin, B. Qi and D. W. Pang, *Adv. Mater.*, 2011, **23**, 5801–5806.
11 J. Deng, Q. Lu, N. Mi, H. Li, M. Liu, M. Xu, L. Tan, Q. Xie, Y. Zhang and S. Yao, *Chemistry*, 2014, **20**, 4993–4999.
12 Y. Hou, Q. Lu, J. Deng, H. Li and Y. Zhang, *Anal. Chim. Acta*, 2015, **866**, 69–74.
13 L. Zeng, X. Li, S. Fan, J. Li, J. Mu, M. Qin, L. Wang, G. Gan, M. Tade and S. Liu, *Nanoscale*, 2019, **11**, 4428–4437.
14 Q. Wang, H. Zheng, Y. Long, L. Zhang, M. Gao and W. Bai, *Carbon*, 2011, **49**, 3134–3140.
15 J. Zheng, Y. Wang, F. Zhang, Y. Yang, X. Liu, K. Guo, H. Wang and B. Xu, *J. Mater. Chem. C*, 2017, **5**, 8105–8111.
16 Z. C. Yang, M. Wang, A. M. Yong, S. Y. Wong, X. H. Zhang, H. Tan, A. Y. Chang, X. Li and J. Wang, *Chem. Commun.*, 2011, **47**, 11615–11617.
17 W. Chen, C. Hu, Y. Yang, J. Cui and Y. Liu, *Materials*, 2016, **9**, 184–191.
18 M. Zhang, L. Hu, H. Wang, Y. Song, Y. Liu, H. Li, M. Shao, H. Huang and Z. Kang, *Nanoscale*, 2018, **10**, 12734–12742.
19 T. V. de Medeiros, J. Manioudakis, F. Noun, J.-R. Macairan, F. Victoria and R. Naccache, *J. Mater. Chem. C*, 2019, **7**, 7175–7195.
20 S. Mitra, S. Chandra, T. Kundu, R. Banerjee, P. Pramanik and A. Goswami, *RSC Adv.*, 2012, **2**, 12129–12131.
21 A. Jaiswal, S. S. Ghosh and A. Chattopadhyay, *Chem. Commun.*, 2012, **48**, 407–409.
22 X. Zhai, P. Zhang, C. Liu, T. Bai, W. Li, L. Dai and W. Liu, *Chem. Commun.*, 2012, **48**, 7955–7957.
23 Z. Ma, H. Ming, H. Huang, Y. Liu and Z. Kang, *New J. Chem.*, 2012, **36**, 861–864.
24 H. Dang, L.-K. Huang, Y. Zhang, C.-F. Wang and S. Chen, *Ind. Eng. Chem. Res.*, 2016, **55**, 5335–5341.
25 J. Zhou, Z. Sheng, H. Han, M. Zou and C. Li, *Mater. Lett.*, 2012, **66**, 222–224.
26 Y. Zhuo, H. Miao, D. Zhong, S. Zhu and X. Yang, *Mater. Lett.*, 2015, **139**, 197–200.
27 Y. Dong, H. Pang, H. B. Yang, C. Guo, J. Shao, Y. Chi, C. M. Li and T. Yu, *Angew. Chem., Int. Ed. Engl.*, 2013, **52**, 7800–7804.
28 Y. H. Yuan, Z. X. Liu, R. S. Li, H. Y. Zou, M. Lin, H. Liu and C. Z. Huang, *Nanoscale*, 2016, **8**, 6770–6776.
29 L. Li and T. Dong, *J. Mater. Chem. C*, 2018, **6**, 7944–7970.
30 J. Zhang, Y. Yuan, G. Liang and S. H. Yu, *Adv. Sci.*, 2015, **2**, 1500002.
31 F. Wang, S. Pang, L. Wang, Q. Li, M. Kreiter and C.-y. Liu, *Chem. Mater.*, 2010, **22**, 4528–4530.
32 C.-C. Huang, Y.-S. Hung, Y.-M. Weng, W. Chen and Y.-S. Lai, *Trends Food Sci. Technol.*, 2019, **86**, 144–152.
33 C. Zhu, J. Zhai and S. Dong, *Chem. Commun.*, 2012, **48**, 9367–9369.
34 Y. Liu, Y. Zhao and Y. Zhang, *Sens. Actuators, B*, 2014, **196**, 647–652.
35 M. Jayanthi, S. Megarajan, S. B. Subramaniyan, R. K. Kamlekar and A. Veerappan, *J. Mol. Liq.*, 2019, **278**, 175–182.
36 L. Wang and H. S. Zhou, *Anal. Chem.*, 2014, **86**, 8902–8905.
37 S. M. Mandal, T. K. Sinha, A. K. Katiyar, S. Das, M. Mandal and S. Ghosh, *J. Nanosci. Nanotechnol.*, 2019, **19**, 6961–6964.
38 J. Guo, D. Liu, I. Filpponen, L. S. Johansson, J. M. Malho, S. Quraishi, F. Liebner, H. A. Santos and O. J. Rojas, *Biomacromolecules*, 2017, **18**, 2045–2055.
39 J. J. Cronican, D. B. Thompson, K. T. Beier, B. R. McNaughton, C. L. Cepko and D. R. Liu, *ACS Chem. Biol.*, 2010, **5**, 747–752.
40 L. Cao, X. Wang, M. J. Meziani, F. Lu, H. Wang, P. G. Luo, Y. Lin, B. A. Harruff, L. M. Veca, D. Murray, S. Y. Xie and Y. P. Sun, *J. Am. Chem. Soc.*, 2007, **129**, 11318–11319.
41 V. S. Sivasankarapillai, J. Jose, M. S. Shanavas, A. Marathakam, M. S. Uddin and B. Mathew, *Curr. Drug Targets*, 2019, **20**, 1255–1263.
42 S. Sahu, B. Behera, T. K. Maiti and S. Mohapatra, *Chem. Commun.*, 2012, **48**, 8835–8837.
43 B. B. Chen, X. Y. Wang and R. C. Qian, *Chem. Commun.*, 2019, **55**, 9681–9684.
44 C. Liu, P. Zhang, F. Tian, W. Li, F. Li and W. Liu, *J. Mater. Chem.*, 2011, **21**, 13163–13167.
45 C. Liu, P. Zhang, X. Zhai, F. Tian, W. Li, J. Yang, Y. Liu, H. Wang, W. Wang and W. Liu, *Biomaterials*, 2012, **33**, 3604–3613.
46 H. Tao, K. Yang, Z. Ma, J. Wan, Y. Zhang, Z. Kang and Z. Liu, *Small*, 2012, **8**, 281–290.
47 B. Chen, F. Li, S. Li, W. Weng, H. Guo, T. Guo, X. Zhang, Y. Chen, T. Huang, X. Hong, S. You, Y. Lin, K. Zeng and S. Chen, *Nanoscale*, 2013, **5**, 1967–1971.
48 J. Tang, B. Kong, H. Wu, M. Xu, Y. Wang, Y. Wang, D. Zhao and G. Zheng, *Adv. Mater.*, 2013, **25**, 6569–6574.
49 C. H. Lee, R. Rajendran, M. S. Jeong, H. Y. Ko, J. Y. Joo, S. Cho, Y. W. Chang and S. Kim, *Chem. Commun.*, 2013, **49**, 6543–6545.
50 B. Wu, G. Zhu, A. Dufresne and N. Lin, *ACS Appl. Mater. Interfaces*, 2019, **11**, 16048–16058.
51 Z. Liu, M. Chen, Y. Guo, J. Zhou, Q. Shi and R. Sun, *Chem. Eng. J.*, 2020, **384**, 123260.
52 R. Mohammadinejad, A. Dadashzadeh, S. Moghassemi, M. Ashrafizadeh, A. Dehshahri, A. Pardakhty, H. Sassan, S. M. Sohrevardi and A. Mandegary, *J. Adv. Res.*, 2019, **18**, 81–93.
53 K. Ghosal and A. Ghosh, *Mater. Sci. Eng., C*, 2019, **96**, 887–903.

54 M. Ashrafizadeh, R. Mohammadinejad, S. K. Kailasa, Z. Ahmadi, E. G. Afshar and A. Pardakhty, *Adv. Colloid Interface Sci.*, 2020, **278**, 102123.
55 D. E. Dolmans, D. Fukumura and R. K. Jain, *Nat. Rev. Cancer*, 2003, **3**, 380–387.
56 S. Y. Kwok, N. F. M. Wai, T. S. Y. Wai and S. Yu, *US Pat.*, 62/525, 471, 2019.
57 Y. Choi, S. Kim, M.-H. Choi, S.-R. Ryoo, J. Park, D.-H. Min and B.-S. Kim, *Adv. Funct. Mater.*, 2014, **24**, 5781–5789.
58 M. Thakur, S. Pandey, A. Mewada, V. Patil, M. Khade, E. Goshi and M. Sharon, *J. Drug Delivery*, 2014, **2014**, 282193.
59 T. R. Kuo, S. Y. Sung, C. W. Hsu, C. J. Chang, T. C. Chiu and C. C. Hu, *Anal. Bioanal. Chem.*, 2016, **408**, 77–82.
60 J. Wang, P. Zhang, C. Huang, G. Liu, K. C. Leung and Y. X. Wang, *Langmuir*, 2015, **31**, 8063–8073.
61 T. Dertinger, R. Colyer, G. Iyer, S. Weiss and J. Enderlein, *Proc. Natl. Acad. Sci. U. S. A.*, 2009, **106**, 22287–22292.
62 A. M. Chizhik, S. Stein, M. O. Dekaliuk, C. Battle, W. Li, A. Huss, M. Platen, I. A. Schaap, I. Gregor, A. P. Demchenko, C. F. Schmidt, J. Enderlein and A. I. Chizhik, *Nano Lett.*, 2016, **16**, 237–242.
63 A. Loukanov, R. Sekiya, M. Yoshikawa, N. Kobayashi, Y. Moriyasu and S. Nakabayashi, *J. Phys. Chem. C*, 2016, **120**, 15867–15874.
64 S. Aiyer, R. Prasad, M. Kumar, K. Nirvikar, B. Jain and O. S. Kushwaha, *Appl. Mater. Today*, 2016, **4**, 71–77.
65 K. Bankoti, A. P. Rameshbabu, S. Datta, B. Das, A. Mitra and S. Dhara, *J. Mater. Chem. B*, 2017, **5**, 6579–6592.
66 J. Zhao, F. Li, S. Zhang, Y. An and S. Sun, *New J. Chem.*, 2019, **43**, 6332–6342.
67 N. Xu, J. Du, Q. Yao, H. Ge, H. Li, F. Xu, F. Gao, L. Xian, J. Fan and X. Peng, *Carbon*, 2020, **159**, 74–82.
68 K. Yang, C. Wang, C. Liu, S. Ding, F. Tian and F. Li, *J. Mater. Sci.*, 2018, **54**, 3383–3391.
69 S. Sun, J. Chen, K. Jiang, Z. Tang, Y. Wang, Z. Li, C. Liu, A. Wu and H. Lin, *ACS Appl. Mater. Interfaces*, 2019, **11**, 5791–5803.
70 W. Lu, X. Qin, S. Liu, G. Chang, Y. Zhang, Y. Luo, A. M. Asiri, A. O. Al-Youbi and X. Sun, *Anal. Chem.*, 2012, **84**, 5351–5357.
71 W. Shi, F. Guo, M. Li, Y. Shi, M. Wu and Y. Tang, *J. Alloys Compd.*, 2019, **775**, 511–517.
72 B. Kong, A. Zhu, C. Ding, X. Zhao, B. Li and Y. Tian, *Adv. Mater.*, 2012, **24**, 5844–5848.
73 A. Zhu, Q. Qu, X. Shao, B. Kong and Y. Tian, *Angew. Chem., Int. Ed. Engl.*, 2012, **51**, 7185–7189.
74 Y. Sha, J. Lou, S. Bai, D. Wu, B. Liu and Y. Ling, *Mater. Res. Bull.*, 2013, **48**, 1728–1731.
75 B. Xu, C. Zhao, W. Wei, J. Ren, D. Miyoshi, N. Sugimoto and X. Qu, *Analyst*, 2012, **137**, 5483–5486.
76 S. Qu, H. Chen, X. Zheng, J. Cao and X. Liu, *Nanoscale*, 2013, **5**, 5514–5518.
77 S. N. A. Mohd Yazid, S. F. Chin, S. C. Pang and S. M. Ng, *Microchim. Acta*, 2012, **180**, 137–143.
78 X. Qin, W. Lu, A. M. Asiri, A. O. Al-Youbi and X. Sun, *Sens. Actuators, B*, 2013, **184**, 156–162.
79 C. Yuan, B. Liu, F. Liu, M. Y. Han and Z. Zhang, *Anal. Chem.*, 2014, **86**, 1123–1130.
80 E.-H. Noh, H. Y. Ko, C. H. Lee, M.-S. Jeong, Y. W. Chang and S. Kim, *J. Mater. Chem. B*, 2013, **1**, 4438–4445.
81 X. W. Tan, A. N. B. Romainor, S. F. Chin and S. M. Ng, *J. Anal. Appl. Pyrolysis*, 2014, **105**, 157–165.
82 M. Vedamalai, A. P. Periasamy, C. W. Wang, Y. T. Tseng, L. C. Ho, C. C. Shih and H. T. Chang, *Nanoscale*, 2014, **6**, 13119–13125.
83 L. Shi, Y. Li, X. Li, B. Zhao, X. Wen, G. Zhang, C. Dong and S. Shuang, *Biosens. Bioelectron.*, 2016, **77**, 598–602.
84 P. Shen and Y. Xia, *Anal. Chem.*, 2014, **86**, 5323–5329.
85 H. Nie, M. Li, Q. Li, S. Liang, Y. Tan, L. Sheng, W. Shi and S. X.-A. Zhang, *Chem. Mater.*, 2014, **26**, 3104–3112.
86 C.-I. Wang, W.-C. Wu, A. P. Periasamy and H.-T. Chang, *Green Chem.*, 2014, **16**, 2509–2514.
87 Z. Mohammadpour, A. Safavi and M. Shamsipur, *Chem. Eng. J.*, 2014, **255**, 1–7.
88 J. Zhang, Y. Ma, Y. Du, H. Jiang, D. Zhou and S. Dong, *Appl. Catal., B*, 2017, **209**, 253–264.
89 J. Shen, S. Shang, X. Chen, D. Wang and Y. Cai, *Mater. Sci. Eng., C*, 2017, **76**, 856–864.
90 Y. Kim, G. Jang and T. S. Lee, *ACS Appl. Mater. Interfaces*, 2015, **7**, 15649–15657.
91 B. B. Chen, M. L. Liu, L. Zhan, C. M. Li and C. Z. Huang, *Anal. Chem.*, 2018, **90**, 4003–4009.
92 B. B. Chen, R. S. Li, M. L. Liu, H. Z. Zhang and C. Z. Huang, *Chem. Commun.*, 2017, **53**, 4958–4961.
93 X. Gong, W. Lu, M. C. Paau, Q. Hu, X. Wu, S. Shuang, C. Dong and M. M. Choi, *Anal. Chim. Acta*, 2015, **861**, 74–84.
94 L. Wang, B. Li, F. Xu, X. Shi, D. Feng, D. Wei, Y. Li, Y. Feng, Y. Wang, D. Jia and Y. Zhou, *Biosens. Bioelectron.*, 2016, **79**, 1–8.
95 L. Zhang, Y. Han, J. Zhu, Y. Zhai and S. Dong, *Anal. Chem.*, 2015, **87**, 2033–2036.
96 A. Cayuela, C. Carrillo-Carrion, M. L. Soriano, W. J. Parak and M. Valcarcel, *Anal. Chem.*, 2016, **88**, 3178–3185.
97 Y. Wu, X. Liu, Q. Wu, J. Yi and G. Zhang, *Anal. Chem.*, 2017, **89**, 7084–7089.
98 H. Huang, C. Li, S. Zhu, H. Wang, C. Chen, Z. Wang, T. Bai, Z. Shi and S. Feng, *Langmuir*, 2014, **30**, 13542–13548.
99 T. N. Edison, R. Atchudan, J. J. Shim, S. Kalimuthu, B. C. Ahn and Y. R. Lee, *J. Photochem. Photobiol., B*, 2016, **158**, 235–242.
100 X. Wen, L. Shi, G. Wen, Y. Li, C. Dong, J. Yang and S. Shuang, *Sens. Actuators, B*, 2016, **235**, 179–187.
101 X. Cui, Y. Wang, J. Liu, Q. Yang, B. Zhang, Y. Gao, Y. Wang and G. Lu, *Sens. Actuators, B*, 2017, **242**, 1272–1280.
102 F. Yan, D. Kong, Y. Luo, Q. Ye, Y. Wang and L. Chen, *Mater. Sci. Eng., C*, 2016, **68**, 732–738.
103 S. Pang, Y. Zhang, C. Wu and S. Feng, *Sens. Actuators, B*, 2016, **222**, 857–863.
104 A. Iqbal, Y. Tian, X. Wang, D. Gong, Y. Guo, K. Iqbal, Z. Wang, W. Liu and W. Qin, *Sens. Actuators, B*, 2016, **237**, 408–415.

105 H. Qi, M. Teng, M. Liu, S. Liu, J. Li, H. Yu, C. Teng, Z. Huang, H. Liu, Q. Shao, A. Umar, T. Ding, Q. Gao and Z. Guo, *J. Colloid Interface Sci.*, 2019, **539**, 332–341.
106 D. Long, J. Peng, H. Peng, H. Xian, S. Li, X. Wang, J. Chen, Z. Zhang and R. Ni, *Analyst*, 2019, **144**, 3307–3313.
107 H. Ehtesabi, S. Roshani, Z. Bagheri and M. Yaghoubi-Avini, *J. Environ. Chem. Eng.*, 2019, **7**, 103419.
108 M. L. Yola and N. Atar, *Composites, Part B*, 2019, **175**, 107113.
109 Y. Fu, S. Zhao, S. Wu, L. Huang, T. Xu, X. Xing, M. Lan and X. Song, *Dyes Pigm.*, 2020, **172**, 107846.
110 R. Jalili, A. Khataee, M. R. Rashidi and A. Razmjou, *Food Chem.*, 2020, **314**, 126172.
111 M. Poshteh Shirani, B. Rezaei and A. A. Ensafi, *Spectrochim. Acta, Part A*, 2019, **210**, 36–43.
112 L. Cai, Z. Fu and F. Cui, *J. Fluoresc.*, 2020, **30**, 11–20.
113 L. Liu, S. Anwar, H. Ding, M. Xu, Q. Yin, Y. Xiao, X. Yang, M. Yan and H. Bi, *J. Electroanal. Chem.*, 2019, **840**, 84–92.
114 J. Wang, Z. Wu, S. Chen, R. Yuan and L. Dong, *Microchem. J.*, 2019, **151**, 104246.
115 J. Y. Liang, L. Han, S. G. Liu, Y. J. Ju, N. B. Li and H. Q. Luo, *Spectrochim. Acta, Part A*, 2019, **222**, 117260.
116 H. J. Lee, J. Jana, J. S. Chung and S. H. Hur, *Dyes Pigm.*, 2020, **175**, 108126.
117 S. Ahmadian-Fard-Fini, D. Ghanbari and M. Salavati-Niasari, *Composites, Part B*, 2019, **161**, 564–577.
118 H. Ming, Z. Ma, Y. Liu, K. Pan, H. Yu, F. Wang and Z. Kang, *Dalton Trans.*, 2012, **41**, 9526–9531.
119 P. Zhou, J. Yu and M. Jaroniec, *Adv. Mater.*, 2014, **26**, 4920–4935.
120 P. Yang, J. Zhao, J. Wang, H. Cui, L. Li and Z. Zhu, *RSC Adv.*, 2015, **5**, 21332–21335.
121 Y. Jiao, Q. Huang, J. Wang, Z. He and Z. Li, *Appl. Catal., B*, 2019, **247**, 124–132.
122 A. Mehta, A. Mishra, S. Basu, N. P. Shetti, K. R. Reddy, T. A. Saleh and T. M. Aminabhavi, *J. Environ. Manage.*, 2019, **250**, 109486.
123 G. Gao, Y. Jiao, F. Ma, Y. Jiao, E. Waclawik and A. Du, *Phys. Chem. Chem. Phys.*, 2015, **17**, 31140–31144.
124 S. Y. Park, H. U. Lee, Y. C. Lee, S. Choi, D. H. Cho, H. S. Kim, S. Bang, S. Seo, S. C. Lee, J. Won, B. C. Son, M. Yang and J. Lee, *Sci. Rep.*, 2015, **5**, 12420.
125 P. Yang, J. Zhao, L. Zhang, L. Li and Z. Zhu, *Chemistry*, 2015, **21**, 8561–8568.
126 B. Song, T. Wang, H. Sun, Q. Shao, J. Zhao, K. Song, L. Hao, L. Wang and Z. Guo, *Dalton Trans.*, 2017, **46**, 15769–15777.
127 Q. Liu, T. Chen, Y. Guo, Z. Zhang and X. Fang, *Appl. Catal., B*, 2017, **205**, 173–181.
128 W.-J. Ong, L. K. Putri, Y.-C. Tan, L.-L. Tan, N. Li, Y. H. Ng, X. Wen and S.-P. Chai, *Nano Res.*, 2017, **10**, 1673–1696.
129 P. Zhang, T. Wang, X. Chang, L. Zhang and J. Gong, *Angew. Chem., Int. Ed. Engl.*, 2016, **55**, 5851–5855.
130 R. Aggarwal, D. Saini, B. Singh, J. Kaushik, A. K. Garg and S. K. Sonkar, *Sol. Energy*, 2020, **197**, 326–331.
131 Z. Zhu, P. Yang, X. Li, M. Luo, W. Zhang, M. Chen and X. Zhou, *Spectrochim. Acta, Part A*, 2020, **227**, 117659.
132 S. Cailotto, M. Negrato, S. Daniele, R. Luque, M. Selva, E. Amadio and A. Perosa, *Green Chem.*, 2020, **22**, 1145–1149.
133 E. Amadio, S. Cailotto, C. Campalani, L. Branzi, C. Raviola, D. Ravelli, E. Cattaruzza, E. Trave, A. Benedetti, M. Selva and A. Perosa, *Molecules*, 2019, **25**, 101.